


Am J Physiol Renal Physiol. 2017 Jan 1; 312(1): F25–F32.

PMCID: PMC5283885

Published online 2016 Oct 19. doi: [10.1152/ajprenal.00311.2016](https://doi.org/10.1152/ajprenal.00311.2016)PMID: [27760767](https://pubmed.ncbi.nlm.nih.gov/27760767/)

Mechanism and Treatment of Renal Fibrosis

Mesenchymal stem cells protect against obstruction-induced renal fibrosis by decreasing STAT3 activation and STAT3-dependent MMP-9 production

[Futoshi Matsui](#),¹ [Stephen A. Babitz](#),² [Audrey Rhee](#),¹ [Karen L. Hile](#),¹ [Hongji Zhang](#),¹ and [Kirstan K. Meldrum](#)^{1,2}¹Department of Urology, Indiana University School of Medicine, Indianapolis, Indiana; and²Division of Pediatric Urology, Helen DeVos Children's Hospital, Grand Rapids, Michigan Corresponding author.Address for reprints and other correspondence: K. K. Meldrum, Michigan State University, Division of Pediatric Urology, Helen DeVos Children's Hospital, 100 Michigan St. SE, Grand Rapids, MI 49503 (e-mail: Kirstan.Meldrum@helendevoschildrens.org).

Received 2016 May 24; Revised 2016 Sep 29; Accepted 2016 Oct 12.

[Copyright](#) © 2017 the American Physiological Society

Abstract

[Go to:](#)

STAT3 is a transcription factor implicated in renal fibrotic injury, but the role of STAT3 in mesenchymal stem cell (MSC)-induced renoprotection during renal fibrosis remains unknown. We hypothesized that MSCs protect against obstruction-induced renal fibrosis by downregulating STAT3 activation and STAT3-induced matrix metalloproteinase-9 (MMP-9) expression. Male Sprague-Dawley rats underwent renal arterial injection of vehicle or MSCs (1×10^6 /rat) immediately before sham operation or induction of unilateral ureteral obstruction (UUO). The kidneys were harvested after 4 wk and analyzed for collagen I and III gene expression, collagen deposition (Masson's trichrome), fibronectin, α -smooth muscle actin, active STAT3 (p-STAT3), MMP-9, and tissue inhibitor of matrix metalloproteinases 1 (TIMP-1) expression. In a separate arm, the STAT3 inhibitor S3I-201 (10 mg/kg) vs. vehicle was administered to rats intraperitoneally just after induction of UUO and daily for 14 days thereafter. The kidneys were harvested after 2 wk and analyzed for p-STAT3 and MMP-9 expression, and collagen and fibronectin deposition. Renal obstruction induced a significant increase in collagen, fibronectin, α -SMA, p-STAT3, MMP-9, and TIMP-1 expression while exogenously administered MSCs significantly reduced these indicators of obstruction-induced renal fibrosis. STAT3 inhibition with S3I-201 significantly reduced obstruction-induced MMP-9 expression and tubulointerstitial fibrosis. These results demonstrate that MSCs protect against obstruction-induced renal fibrosis, in part, by decreasing STAT3 activation and STAT3-dependent MMP-9 production.

Keywords: mesenchymal stem cell, signal transducers and activators of transcription, matrix metalloproteinases, kidney, unilateral ureteral obstruction, epithelial mesenchymal transition, ureteral obstruction, matrix metalloproteinase-9, signal transducer and activator of transcription-3

MESENCHYMAL STEM CELLS (MSCs) are nonembryonic stem cells of mesodermal origin that have the capacity to differentiate into cells of connective tissue lineage and have a unique ability to home or migrate to injured tissue (1, 8, 28). MSCs are anti-inflammatory and can inhibit immune cell activation and proliferation, as well as the production of proinflammatory mediators (1, 8, 28). Several studies have

demonstrated that MSCs can protect against acute and chronic renal injury (1, 8, 28), and, while the mechanism of MSC-induced renal protection remains unknown, recent studies suggest that a significant component of MSC's protective and reparative function resides in their paracrine activity. MSCs can secrete a number of growth factors and cytokines that are important for angiogenesis and cytoprotection and have been demonstrated to prevent tubulointerstitial fibrosis during chronic unilateral ureteral obstruction (UUO) (2, 5, 9).

Progressive tubulointerstitial fibrosis is a prominent characteristic of obstruction-induced renal injury and represents the final common pathway for nearly all forms of chronic kidney disease (CKD). Interstitial fibrosis is characterized by a prominent inflammatory cell infiltrate, fibroblast proliferation, and an imbalance in extracellular matrix (ECM) synthesis and degradation (7, 15, 25). The release of a number of cytokines and growth factors during obstructive renal injury induces profibrotic signaling, reduces ECM degradation, and stimulates renal tubular cell epithelial mesenchymal transition (EMT), a process by which tubular epithelial cells (TECs) undergo a phenotypic transformation into matrix-producing fibroblasts (11, 29, 30, 44).

Matrix metalloproteinases (MMPs) are a large family of endopeptidases that proteolyze all components of ECM and are critical for ECM remodeling and matrix homeostasis. MMP activity is regulated by the tissue inhibitors of matrix metalloproteinases (TIMPs), a family of specific endogenous inhibitors of MMPs that bind MMPs in a 1:1 stoichiometry. MMPs are traditionally believed to have an antifibrotic role in the development and progression of CKD because of their proteolytic activity (33); however, recent studies have demonstrated that MMPs, particularly MMP-9, can stimulate renal fibrosis and EMT during obstructive renal injury (33, 41). MMP-9 has been shown to mediate EMT in tubular epithelial cells in vitro (34, 45), and recent reports link MMP-9 expression in mammary epithelial cells and dermal fibroblasts to STAT3 activation (6, 40).

The JAK/STAT signaling pathway has increasingly been implicated in the pathophysiology of fibrotic renal disease (19), and STAT3 has been demonstrated to have a significant role in obstruction-induced tubulointerstitial fibrosis and profibrotic signaling in TECs in vitro (20, 23). Whereas MSCs have been demonstrated to improve left ventricular function and activate cardiac repair mechanisms in the diseased heart through STAT3 signaling (27), the relationship between STAT3 and MMP-9 during renal obstruction and the role of STAT3 and MMP-9 in MSC-induced renoprotection remains unknown. We therefore hypothesized that MSCs protect against obstruction-induced renal fibrosis by reducing STAT3 activation and STAT3-dependent MMP-9 production. To study this, renal cortical collagen I and III gene expression, fibronectin, α -smooth muscle actin (α -SMA), active STAT3 (p-STAT3), MMP-9, and TIMP-1 expression were examined in Sprague-Dawley rats using a well-established model of UUO. In addition, the effect of STAT3 inhibition on obstruction-induced MMP-9 expression and tubulointerstitial fibrosis was evaluated.

MATERIALS AND METHODS

[Go to:](#)

Animals, experimental groups, operative techniques, and S3I-201 treatment. The animal protocol was reviewed and accepted by the Animal Care and Research Committee of the Indiana University School of Medicine. Adult male Sprague-Dawley rats weighing 250–300 g were acclimated and maintained on a standard pellet diet for 1 wk before experiment initiation. The animals were anesthetized with isoflurane inhalation. Human MSCs were purchased from Cambrex Bio Science Walkersville (Walkersville, MD) and cultured in MSC Basal Medium (Lonza, Walkersville, MD) containing 10% fetal bovine serum for 14 days before injection. According to the manufacturer, cells are positive for CD105, CD166, CD29, and CD44 and negative for CD14, CD34, and CD45. MSCs were labeled with the PKH26 red fluorescence cell linker kit (Sigma-Aldrich, St. Louis, MO) according to the manufacturer's protocol, just before injection. Following the induction of anesthesia, rats underwent renal arterial injection of either vehicle or MSCs ($1 \times$

10⁶/rat) according to the techniques previously described (16). Subsequently, the left ureter was completely ligated with 5–0 silk suture. Sham-operated rats underwent an identical surgical procedure without ureteral ligation. The animals underwent renal arterial injection of MSCs or vehicle immediately before UUO and were subjected to 4 wk of obstruction vs. sham operation. Four weeks postoperatively, rats were anesthetized, the left kidneys were removed and snap-frozen in liquid nitrogen, and the animals were subsequently killed. The animals were divided into four experimental groups (6 animals/group) as follows: sham operation, UUO plus vehicle, sham plus MSCs, and UUO plus MSCs.

In the separate arm, the specific STAT3 inhibitor S3I-201 (10 mg/kg; EMD Chemicals, San Diego, CA) (23) or vehicle (0.05% DMSO) was administered to rats intraperitoneally just after induction of UUO and daily for 14 days thereafter. Rats were subjected to 2 wk of obstruction vs. sham operation. After 2 wk, rats were killed, the left kidneys were removed and snap-frozen in liquid nitrogen, and the animals were subsequently killed. The animals were divided into three experimental groups (6 animals/group) as follows: sham operation, UUO plus vehicle, and UUO plus S3I-201.

Tissue homogenization. A portion of each renal cortex was homogenized after the samples had been diluted in 10 vol of homogenate buffer/g of tissue [10 mM HEPES (pH 7.9), 10 mM KCl, 0.1 mM EGTA, 0.1 mM DTT, and Complete Protease Inhibitor tabs (Roche Diagnostics, Indianapolis, IN)] using a vertishear tissue homogenizer. Renal homogenates were then centrifuged at 3,000 g for 15 min at 4°C, and the supernatants were stored at –80°C until the ELISAs or Western blots could be performed.

Real-time PCR. Total RNA was extracted from renal cortical tissue by homogenization in Trizol (GIBCO-BRL, Gaithersburg, MD) and then isolated by precipitation with chloroform and isopropanol. Total RNA (0.5 µg) was subjected to cDNA synthesis using iScript (Bio-Rad, Hercules, CA). The cDNA from each sample was analyzed for collagen 1a2 (Rn01526724_m1), collagen 3a1 (Rn01437681_m1), and MMP-9 (Rn00579162_m1) using *TaqMan* gene expression assay (RT-PCR; Applied Biosystems, Foster City, CA). FAM/Dye MGB-labeled probes for rat β-actin (Applied Biosystems) served as endogenous controls.

Masson's trichrome staining. Tissue sections (4 µm) were deparaffinized and rehydrated with alcohol. The slides were then washed in distilled water and stained in Weigert's iron hematoxylin working solution for 10 min. The slides were washed and stained in Biebrich scarlet-acid fuchsin solution for 15 min. The slides were then rewashed and differentiated in phosphomolybdic-phosphotungstic acid solution for 15 min. The tissue sections were then transferred directly to aniline blue solution for 5–10 min, rinsed, and differentiated in 1% acetic acid solution for 2–5 min. The slides were dehydrated, cleared in xylene, and mounted.

Fibronectin and α-SMA tissue staining. Renal sections (4 µm) were harvested from each sample, fixed in 4% PFA/PBS, and placed in paraffin. After deparaffinization, antigen retrieval was conducted on slides. Sections were exposed to a Biocare reveal decloaker for 30 min at 90°C, washed in TBS three times, incubated for 30 min in rodent block M blocking solution, and incubated for 5 min in background punisher. Slides were then incubated with anti-fibronectin antibody ab2413 (1:200; Abcam Cambridge, MA) or anti-α-SMA antibody (1A4 clone) (1:200; Santa Cruz, Dallas, TX) for 2 h at room temperature (RT). Slides were washed three times in TBS and incubated for 45 min at RT with a 4+ HRP detection kit (Biocare Medical, Concord, CA). The slides were counterstained with CAT hematoxylin. To assess immunostaining specificity, adjacent sections were incubated without primary antibody and processed using identical conditions. Slides were mounted and imaged at ×400 using a Nikon Eclipse microscope and Nikon digital imager (Nikon, Tokyo, Japan).

STAT3 tissue staining. Tissue sections (4 µm) were deparaffinized and dehydrated with xylene and alcohol. Antigen was retrieved by incubating the cells with proteinase K for 20 min in an oven. The tissues were then blocked with 1% bovine serum albumin. Slides were incubated with an anti-p-STAT3(Tyr⁷⁰⁵)

antibody (1:25; Cell Signaling, Danvers, MA) for 30 min. The slides were washed in TBS and incubated with the secondary antibody (goat anti-rabbit; Dako EnVision, Carpinteria, CA) for 30 min. Peroxidase-stained sections were then developed with 3,3'-diaminobenzidine and counterstained with hemalum. Sections incubated without primary antibody exhibited no staining.

Western blot analysis. Protein extracts from homogenized samples (30 µg/lane) were subjected to SDS-PAGE on a Tris-glycine gel and transferred to a polyvinylidene fluoride membrane. Immunoblotting was performed by incubating each membrane in 5% dry milk for 1 h, followed by incubation with an anti- α -SMA monoclonal antibody (clone 1A4, 1:500 overnight at 4°C; R&D Systems, Minneapolis, MN), an anti-p-STAT3 antibody (1:200 overnight at 4°C; Cell Signaling), or an anti-fibronectin antibody (1:200 overnight at 4°C; Santa Cruz Biotechnology). After being washed three times in TBST, each membrane was incubated for 1 h at RT with a peroxidase-conjugated secondary antibody (1:2,000). Equivalent protein loading in each lane was confirmed by stripping and reblotting each membrane for GAPDH (1:10,000 for 30 min at RT, secondary 1:10,000 for 30 min at RT; Biodesign, Saco, ME). The membranes were developed using enhanced chemiluminescence (Amersham Pharmacia Biotech, Piscataway, NJ), and the density of each band was determined using National Institutes of Health image analysis software and expressed as a percentage of GAPDH density.

ELISA. Renal cortical homogenate total MMP-9 and TIMP-1 protein levels were determined using an ELISA. The ELISA was performed by adding 100 µl of each sample to wells in a 96-well plate of a rat ELISA kit (MMP-9 and TIMP-1; R&D Systems). Each ELISA was performed according to manufacturer instructions. Final results were expressed as nanograms of MMP-9 or TIMP-1 per milligram protein.

Statistical analysis. Data are presented as means \pm SE. Differences at the 95% confidence level were considered significant. The experiment groups were compared using one-way ANOVA with post hoc Bonferroni-Dunn (JMP 11).

RESULTS

[Go to:](#)

Collagen, fibronectin, and α -SMA expression. To evaluate the effect of exogenously delivered MSCs on obstruction-induced renal fibrosis, collagen mRNA expression and renal cortical Masson's trichrome staining were evaluated in response to 4 wk of obstruction. Collagen I and collagen III mRNA expression ([Fig. 1, A and B](#)) and tubulointerstitial collagen deposition ([Fig. 1C](#)) significantly increased in response to 4 wk of obstruction; however, obstruction-induced collagen expression and deposition were markedly reduced in the presence of exogenous MSCs.

Similarly, fibronectin and α -SMA expression were significantly increased in response to 4 wk of obstruction ([Fig. 2](#)) but reduced to near sham treatment levels in the presence of MSCs. Fibronectin deposition primarily localized to the glomerulus in sham-treated animals and MSC-treated animals subjected to obstruction, whereas animals exposed to 4 wk of obstruction in the absence of MSCs demonstrated increased fibronectin deposition in the tubulointerstitial compartment and glomerulus. Renal cortical α -SMA deposition was also significantly increased in response to 4 wk of obstruction and exhibited a tubulointerstitial pattern of distribution in obstructed samples with only arteriolar staining evident in sham samples ([Fig. 2](#)). In contrast, α -SMA deposition in the tubulointerstitial compartment was minimal in MSC-treated animals exposed to 4 wk of obstruction ([Fig. 3](#)).

MMP-9 and TIMP-1 expression. Renal cortical MMP-9 protein and mRNA levels were minimal in sham-treated animals but increased significantly in response to 4 wk of obstruction. In the presence of exogenously delivered MSCs, obstruction-induced MMP-9 levels were dramatically reduced to near sham treatment levels ([Fig. 4, A and B](#)). Similarly, TIMP-1 expression was significantly increased in response to 4 wk of obstruction but reduced in the presence of MSCs ([Fig. 4C](#)). Whereas TIMP-1 expression was

significantly reduced in the presence of MSCs, an analysis of the ratio of TIMP-1/MMP-9 expression in each sample demonstrated over an eightfold increase in TIMP-1/MMP-9 expression in obstructed animals treated with MSCs compared with vehicle-treated animals (Fig. 4D). These findings suggest that MSCs protect against obstruction-induced renal fibrosis by dramatically reducing MMP-9 expression and causing a significant increase in the ratio of TIMP-1 to MMP-9 expression.

STAT3 activation. To evaluate the effect of MSCs on obstruction-induced STAT3 activation, p-STAT3 expression and the immunohistochemical localization of p-STAT3 were evaluated in renal cortical tissue samples. p-STAT3 expression and the number of nuclei staining positive for p-STAT3 increased significantly in response to 4 wk of obstruction (Fig. 5, A and B), with nuclear p-STAT3 staining localizing primarily to renal tubular epithelial cells and interstitial cells. In contrast, obstruction-induced p-STAT3 expression and nuclear staining for p-STAT3 were significantly reduced in the presence of exogenously delivered MSCs.

Relationship between STAT3 activation and MMP-9 expression. To evaluate the relationship between MMP-9 expression and STAT3 activation, MMP-9 expression levels were evaluated in animals subjected to 2 wk of UUO in the presence of STAT3 inhibition (S3I-201) or vehicle. S3I-201 significantly reduced STAT3 activation in response to obstruction (Fig. 6A) and, further, was demonstrated to significantly reduce renal MMP-9 expression levels in response to obstruction (Fig. 6B). These findings suggest that obstruction-induced MMP-9 expression is, in part, dependent on STAT3 activation.

Impact of STAT3 inhibition on collagen and fibronectin deposition. To evaluate the impact of STAT3 inhibition on obstruction-induced tubulointerstitial fibrosis and the deposition of collagen and fibronectin, renal cortical tissue sections were stained for collagen with Masson's trichrome and for fibronectin. Both collagen deposition and fibronectin staining were significantly increased in the tubulointerstitial compartment of the kidney in response to 2 wk of obstruction (Fig. 7). Animals exposed to STAT3 inhibition, however, demonstrated a marked reduction in collagen and fibronectin deposition in response to obstruction.

DISCUSSION

[Go to:](#)

Mesenchymal stem cell-based therapies have been shown to confer renal protection in several models of acute kidney injury (AKI) (10, 12–14, 21, 35, 36, 46), and early clinical trials have demonstrated the safety and efficacy of MSCs in protecting against renal dysfunction and reducing both the length of stay and need for hospital readmission in cardiac surgery patients at high risk for postoperative AKI (37, 42). A decreased incidence of acute rejection has also been demonstrated in patients receiving MSCs at the time of kidney transplantation (32). Although MSC therapy is becoming an attractive strategy for renal repair, most clinical trials involve only early phases of kidney disease (28), and the potential of MSC-based therapy to prevent or ameliorate CKD is only beginning to be elucidated. Several recent animal studies show the capacity of exogenously administered MSCs to dramatically reduce tubulointerstitial fibrosis, preserve peritubular capillary density, and prevent epithelial mesenchymal transition in multiple different models of chronic renal injury (2, 3, 5, 22, 26, 31, 38). Our results support these observations and demonstrate a significant reduction in obstruction-induced collagen I and III mRNA expression, collagen deposition, fibronectin and α -SMA expression, and fibronectin and α -SMA deposition in the kidney in the presence of MSCs.

Whereas the specific mechanism of MSC-induced renoprotection remains unknown, accumulating evidence suggests that exogenously administered stem cells mediate their renoprotective effect through paracrine activity, since MSC-conditioned medium appears to be as effective as injected cells in protecting against kidney injury (5, 18, 24). The specific mediator or mediators responsible for MSC-induced renoprotection, however, remains to be determined. In an obstructive model of CKD, MSCs have been

shown to decrease renal TNF- α expression but not effect transforming growth factor (TGF)- β 1, VEGF, IL-10, FGF, or hepatocyte growth factor expression (2), whereas, in a model of diabetic nephropathy, MSCs appear to reduce renal TGF- β 1 expression and signaling while increasing renal BMP-7 production (18, 24). MSCs have also been demonstrated to increase renal hepatocyte growth factor production in a 5/6 nephrectomy model of CKD (4).

Many of the profibrotic cytokines and growth factors released during CKD are sequestered in the extracellular matrix in a quiescent state but can be released and made more bioavailable to neighboring cells with the activity of proteinases such as MMP-9.

MMP-9 is a gelatinase that digests denatured collagens and is critical for ECM remodeling and matrix homeostasis. While MMP-9 was traditionally thought to have an antifibrotic role in renal fibrosis due to its proteolytic activity (33), evidence suggests that MMP-9 is an important mediator of renal fibrosis and EMT during obstructive renal injury independent of TGF- β expression (41). MMP-9 is upregulated in response to kidney obstruction and has been shown to promote EMT by stimulating E-cadherin shedding and tubular basement membrane degradation (41, 45). It can also release and activate a variety of profibrotic growth factors and cytokines sequestered in the ECM upon proteolysis (39). Because MSCs appear to have a heterogeneous effect on cytokine expression and signaling during CKD, depending on the model of injury, we sought to investigate the effect of MSCs on matrix regulation as a potential explanation for this variable response.

Our results demonstrate a dramatic reduction in obstruction-induced MMP-9 and TIMP-1 expression, and over an eightfold increase in the ratio of TIMP-1 to MMP-9 expression, in the presence of MSCs. These results support prior observations in the literature that MMP-9 and TIMP-1 expression are increased in response to obstruction (41, 43) and provide the first report that exogenously delivered MSCs may stimulate renal protection by reducing MMP-9 expression. Whereas injected MSCs release an array of protective cytokines and growth factors that likely contribute to renal repair, these results suggest that another important mechanism of MSC-induced renoprotection may involve a dramatic reduction in MMP-9-mediated profibrotic mediator release from the ECM and a subsequent reduction in the activation and bioavailability of these cytokines and growth factors. This effect of MSCs on matrix regulation and MMP-9 expression could also explain the significant anti-fibrotic properties of MSCs observed during kidney obstruction despite persistently elevated TGF- β and FGF expression.

Recent reports link MMP-9 expression in mammary epithelial cells and dermal fibroblasts to STAT3 activation (6, 40), and STAT3 has previously been shown to mediate profibrotic signaling in TECs (17, 20) and tubulointerstitial fibrosis in response to kidney obstruction (17, 23). Despite STAT3's significant role in obstruction-induced renal injury, the effect of MSCs on obstruction-induced STAT3 expression has not previously been evaluated. Our results demonstrate that the presence of MSCs stimulates a significant reduction in active STAT3 expression during kidney obstruction and suggests that STAT3 has a significant role in MSC-mediated renoprotection. Given the findings linking MMP-9 expression to STAT3 activation in other cells, we investigated the effect of STAT3 activation on MMP-9 expression and tubulointerstitial fibrosis during kidney obstruction. We found that the specific STAT3 inhibitor S3I-201 (23) significantly reduces active STAT3 and MMP-9 expression in response to kidney obstruction and, further, causes a significant reduction in obstruction-induced tubulointerstitial fibrosis and collagen and fibronectin deposition. These findings not only suggest that STAT3 activation contributes to MMP-9 upregulation and tubulointerstitial fibrosis during kidney obstruction, they suggest that MSCs may reduce MMP-9 expression during UUO through a STAT3-dependent mechanism.

In conclusion, our study demonstrates that MSCs protect against obstruction-induced renal fibrosis and suggest that their mechanism of action may involve a decrease in STAT3 activation and STAT3-dependent MMP-9 production. A greater understanding of the interaction between STAT signaling and MMP

production and the impact of MSCs on matrix regulation during chronic renal injury may facilitate the application of MSCs in the treatment of CKD.

GRANTS

[Go to:](#)

This research was supported by National Institute of Diabetes and Digestive and Kidney Diseases Grant DK-065892 (K. K. Meldrum).

DISCLOSURES

[Go to:](#)

No conflicts of interest, financial or otherwise, are declared by the authors.

AUTHOR CONTRIBUTIONS

[Go to:](#)

F.M., S.B., A.R., K.L.H., and H.Z. performed experiments; F.M., S.B., and K.K.M. interpreted results of experiments; F.M. and K.K.M. prepared figures; F.M. drafted manuscript; F.M., S.B., A.R., K.L.H., H.Z., and K.K.M. approved final version of manuscript; S.B. and K.K.M. analyzed data; K.K.M. conception and design of research; K.K.M. edited and revised manuscript.

REFERENCES

[Go to:](#)

1. Asanuma H, Meldrum DR, Meldrum KK.. Therapeutic applications of mesenchymal stem cells to repair kidney injury. *J Urol* 184: 26–33, 2010. doi:10.1016/j.juro.2010.03.050. [PubMed: 20478602]
2. Asanuma H, Vanderbrink BA, Campbell MT, Hile KL, Zhang H, Meldrum DR, Meldrum KK.. Arterially delivered mesenchymal stem cells prevent obstruction-induced renal fibrosis. *J Surg Res* 168: e51–e59, 2011. doi:10.1016/j.jss.2010.06.022. [PMCID: PMC3008314] [PubMed: 20850784]
3. Bai ZM, Deng XD, Li JD, Li DH, Cao H, Liu ZX, Zhang J.. Arterially transplanted mesenchymal stem cells in a mouse reversible unilateral ureteral obstruction model: in vivo bioluminescence imaging and effects on renal fibrosis. *Chin Med J (Engl)* 126: 1890–1894, 2013. [PubMed: 23673105]
4. Chang JW, Tsai HL, Chen CW, Yang HW, Yang AH, Yang LY, Wang PS, Ng YY, Lin TL, Lee OK.. Conditioned mesenchymal stem cells attenuate progression of chronic kidney disease through inhibition of epithelial-to-mesenchymal transition and immune modulation. *J Cell Mol Med* 16: 2935–2949, 2012. doi:10.1111/j.1582-4934.2012.01610.x. [PMCID: PMC4393722] [PubMed: 22862802]
5. da Silva AF, Silva K, Reis LA, Teixeira VP, Schor N.. Bone Marrow-Derived Mesenchymal Stem Cells and Their Conditioned Medium Attenuate Fibrosis in an Irreversible Model of Unilateral Ureteral Obstruction. *Cell Transplant* 24: 2657–2666, 2015. doi:10.3727/096368915X687534. [PubMed: 25695732]
6. Dechow TN, Pedranzini L, Leitch A, Leslie K, Gerald WL, Linkov I, Bromberg JF.. Requirement of matrix metalloproteinase-9 for the transformation of human mammary epithelial cells by Stat3-C. *Proc Natl Acad Sci USA* 101: 10602–10607, 2004. doi:10.1073/pnas.0404100101. [PMCID: PMC489981] [PubMed: 15249664]
7. Eddy AA. Molecular insights into renal interstitial fibrosis. *J Am Soc Nephrol* 7: 2495–2508, 1996. [PubMed: 8989727]
8. Galderisi U, Giordano A.. The gap between the physiological and therapeutic roles of mesenchymal stem cells. *Med Res Rev* 34: 1100–1126, 2014. doi:10.1002/med.21322. [PubMed: 24866817]
9. Gregorini M, Corradetti V, Rocca C, Pattonieri EF, Valsania T, Milanese S, Serpieri N, Bedino G, Esposito P, Libetta C, Avanzini MA, Mantelli M, Ingo D, Peressini S, Albertini R, Dal Canton A, Rampino T.. Mesenchymal stromal cells prevent renal fibrosis in a rat model of unilateral ureteral obstruction by

suppressing the renin-angiotensin system via HuR. *PLoS One* 11: e0148542, 2016.

doi:10.1371/journal.pone.0148542. [PMCID: PMC4750962] [PubMed: 26866372]

10. Hara Y, Stolk M, Ringe J, Dehne T, Ladhoff J, Kotsch K, Reutzel-Selke A, Reinke P, Volk HD, Seifert M.. In vivo effect of bone marrow-derived mesenchymal stem cells in a rat kidney transplantation model with prolonged cold ischemia. *Transpl Int* 24: 1112–1123, 2011. doi:10.1111/j.1432-2277.2011.01328.x. [PubMed: 21880071]

11. Healy E, Brady HR.. Role of tubule epithelial cells in the pathogenesis of tubulointerstitial fibrosis induced by glomerular disease. *Curr Opin Nephrol Hypertens* 7: 525–530, 1998. doi:10.1097/00041552-199809000-00007. [PubMed: 9818199]

12. Herrera MB, Bussolati B, Bruno S, Fonsato V, Romanazzi GM, Camussi G.. Mesenchymal stem cells contribute to the renal repair of acute tubular epithelial injury. *Int J Mol Med* 14: 1035–1041, 2004. doi:10.3892/ijmm.14.6.1035. [PubMed: 15547670]

13. Herrera MB, Bussolati B, Bruno S, Morando L, Mauriello-Romanazzi G, Sanavio F, Stamenkovic I, Biancone L, Camussi G.. Exogenous mesenchymal stem cells localize to the kidney by means of CD44 following acute tubular injury. *Kidney Int* 72: 430–441, 2007. doi:10.1038/sj.ki.5002334. [PubMed: 17507906]

14. Kim JH, Park DJ, Yun JC, Jung MH, Yeo HD, Kim HJ, Kim DW, Yang JI, Lee GW, Jeong SH, Roh GS, Chang SH.. Human adipose tissue-derived mesenchymal stem cells protect kidneys from cisplatin nephrotoxicity in rats. *Am J Physiol Renal Physiol* 302: F1141–F1150, 2012. doi:10.1152/ajprenal.00060.2011. [PubMed: 22205231]

15. Klahr S. Progression of chronic renal disease. *Heart Dis* 3: 205–209, 2001. doi:10.1097/00132580-200105000-00013. [PubMed: 11975793]

16. Kunter U, Rong S, Djuric Z, Boor P, Müller-Newen G, Yu D, Floege J.. Transplanted mesenchymal stem cells accelerate glomerular healing in experimental glomerulonephritis. *J Am Soc Nephrol* 17: 2202–2212, 2006. doi:10.1681/ASN.2005080815. [PubMed: 16790513]

17. Kuratsune M, Masaki T, Hirai T, Kiribayashi K, Yokoyama Y, Arakawa T, Yorioka N, Kohno N.. Signal transducer and activator of transcription 3 involvement in the development of renal interstitial fibrosis after unilateral ureteral obstruction. *Nephrology (Carlton)* 12: 565–571, 2007. doi:10.1111/j.1440-1797.2007.00881.x. [PubMed: 17995582]

18. Lv S, Liu G, Sun A, Wang J, Cheng J, Wang W, Liu X, Nie H, Guan G.. Mesenchymal stem cells ameliorate diabetic glomerular fibrosis in vivo and in vitro by inhibiting TGF- β signalling via secretion of bone morphogenetic protein 7. *Diab Vasc Dis Res* 11: 251–261, 2014. doi:10.1177/1479164114531300. [PubMed: 24845071]

19. Matsui F, Meldrum KK.. The role of the Janus kinase family/signal transducer and activator of transcription signaling pathway in fibrotic renal disease. *J Surg Res* 178: 339–345, 2012. doi:10.1016/j.jss.2012.06.050. [PMCID: PMC4867197] [PubMed: 22883438]

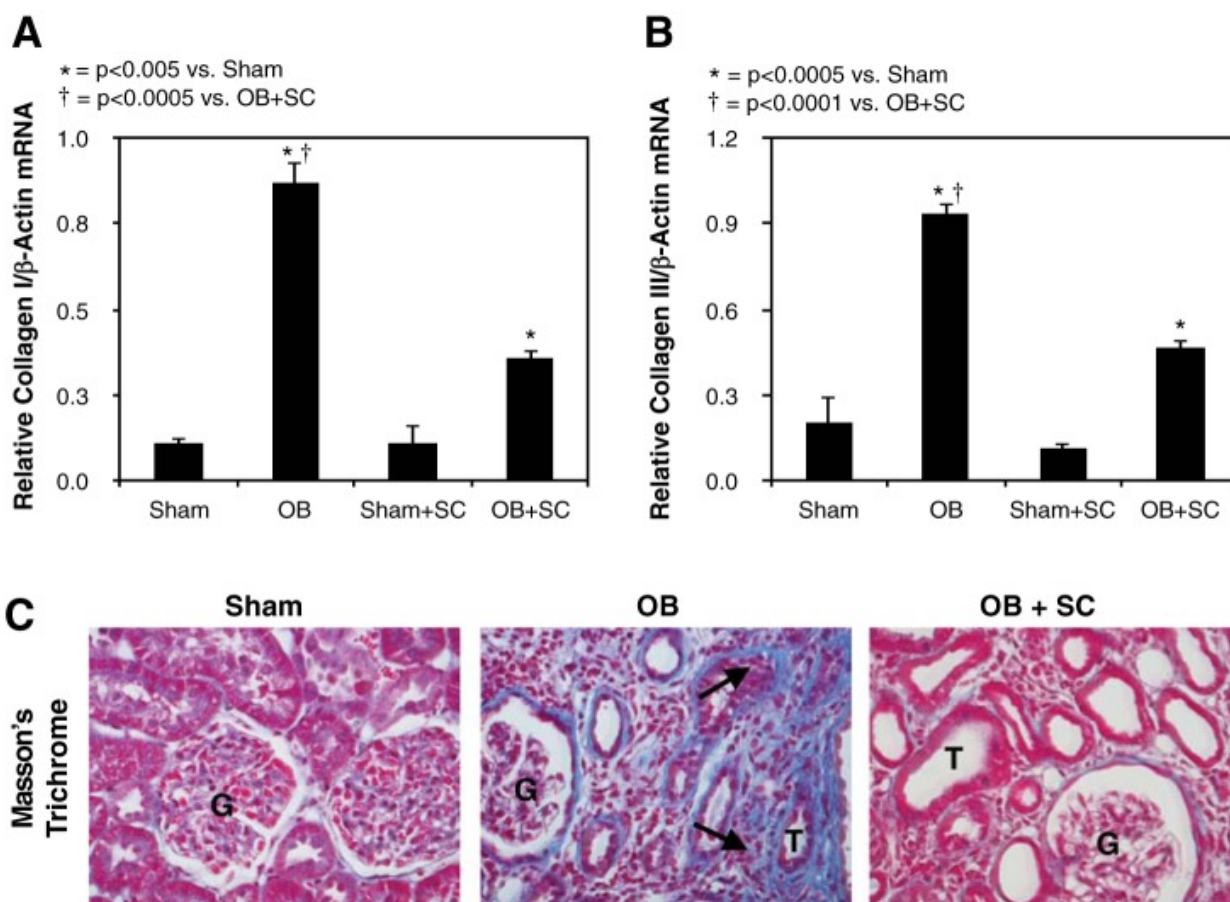
20. Matsui F, Rhee A, Hile KL, Zhang H, Meldrum KK.. IL-18 induces profibrotic renal tubular cell injury via STAT3 activation. *Am J Physiol Renal Physiol* 305: F1014–F1021, 2013. doi:10.1152/ajprenal.00620.2012. [PMCID: PMC4073972] [PubMed: 23904224]

21. Morigi M, Imberti B, Zoja C, Corna D, Tomasoni S, Abbate M, Rottoli D, Angioletti S, Benigni A, Perico N, Alison M, Remuzzi G.. Mesenchymal stem cells are renotropic, helping to repair the kidney and improve function in acute renal failure. *J Am Soc Nephrol* 15: 1794–1804, 2004.

- doi:10.1097/01.ASN.0000128974.07460.34. [PubMed: 15213267]
22. Ninichuk V, Gross O, Segerer S, Hoffmann R, Radomska E, Buchstaller A, Huss R, Akis N, Schlöndorff D, Anders HJ.. Multipotent mesenchymal stem cells reduce interstitial fibrosis but do not delay progression of chronic kidney disease in collagen4A3-deficient mice. *Kidney Int* 70: 121–129, 2006. doi:10.1038/sj.ki.5001521. [PubMed: 16723981]
23. Pang M, Ma L, Gong R, Tolbert E, Mao H, Ponnusamy M, Chin YE, Yan H, Dworkin LD, Zhuang S.. A novel STAT3 inhibitor, S3I-201, attenuates renal interstitial fibroblast activation and interstitial fibrosis in obstructive nephropathy. *Kidney Int* 78: 257–268, 2010. doi:10.1038/ki.2010.154. [PubMed: 20520592]
24. Park JH, Hwang I, Hwang SH, Han H, Ha H.. Human umbilical cord blood-derived mesenchymal stem cells prevent diabetic renal injury through paracrine action. *Diabetes Res Clin Pract* 98: 465–473, 2012. doi:10.1016/j.diabres.2012.09.034. [PubMed: 23026513]
25. Remuzzi G, Bertani T.. Pathophysiology of progressive nephropathies. *N Engl J Med* 339: 1448–1456, 1998. doi:10.1056/NEJM19981123392007. [PubMed: 9811921]
26. Semedo P, Correa-Costa M, Antonio Cenedeze M, Maria Avancini Costa Malheiros D, Antonia dos Reis M, Shimizu MH, Seguro AC, Pacheco-Silva A, Saraiva Camara NO.. Mesenchymal stem cells attenuate renal fibrosis through immune modulation and remodeling properties in a rat remnant kidney model. *Stem Cells* 27: 3063–3073, 2009. doi:10.1002/stem.214. [PubMed: 19750536]
27. Shabbir A, Zisa D, Lin H, Mastro M, Roloff G, Suzuki G, Lee T.. Activation of host tissue trophic factors through JAK-STAT3 signaling: a mechanism of mesenchymal stem cell-mediated cardiac repair. *Am J Physiol Heart Circ Physiol* 299: H1428–H1438, 2010. doi:10.1152/ajpheart.00488.2010. [PMCID: PMC2993206] [PubMed: 20852053]
28. Squillaro T, Peluso G, Galderisi U.. Clinical Trials With Mesenchymal Stem Cells: An Update. *Cell Transplant* 25: 829–848, 2016. doi:10.3727/096368915X689622. [PubMed: 26423725]
29. Strutz F, Müller GA, Neilson EG.. Transdifferentiation: a new angle on renal fibrosis. *Exp Nephrol* 4: 267–270, 1996. [PubMed: 8931981]
30. Strutz F, Okada H, Lo CW, Danoff T, Carone RL, Tomaszewski JE, Neilson EG.. Identification and characterization of a fibroblast marker: FSP1. *J Cell Biol* 130: 393–405, 1995. doi:10.1083/jcb.130.2.393. [PMCID: PMC2199940] [PubMed: 7615639]
31. Sun D, Bu L, Liu C, Yin Z, Zhou X, Li X, Xiao A.. Therapeutic effects of human amniotic fluid-derived stem cells on renal interstitial fibrosis in a murine model of unilateral ureteral obstruction. *PLoS One* 8: e65042, 2013. doi:10.1371/journal.pone.0065042. [PMCID: PMC3665750] [PubMed: 23724119]
32. Tan J, Wu W, Xu X, Liao L, Zheng F, Messinger S, Sun X, Chen J, Yang S, Cai J, Gao X, Pileggi A, Ricordi C.. Induction therapy with autologous mesenchymal stem cells in living-related kidney transplants: a randomized controlled trial. *JAMA* 307: 1169–1177, 2012. doi:10.1001/jama.2012.316. [PubMed: 22436957]
33. Tan RJ, Liu Y.. Matrix metalloproteinases in kidney homeostasis and diseases. *Am J Physiol Renal Physiol* 302: F1351–F1361, 2012. doi:10.1152/ajprenal.00037.2012. [PMCID: PMC3774496] [PubMed: 22492945]
34. Tan TK, Zheng G, Hsu TT, Wang Y, Lee VW, Tian X, Wang Y, Cao Q, Wang Y, Harris DC.. Macrophage matrix metalloproteinase-9 mediates epithelial-mesenchymal transition in vitro in murine renal tubular cells. *Am J Pathol* 176: 1256–1270, 2010. doi:10.2353/ajpath.2010.090188. [PMCID: PMC2832147] [PubMed: 20075196]

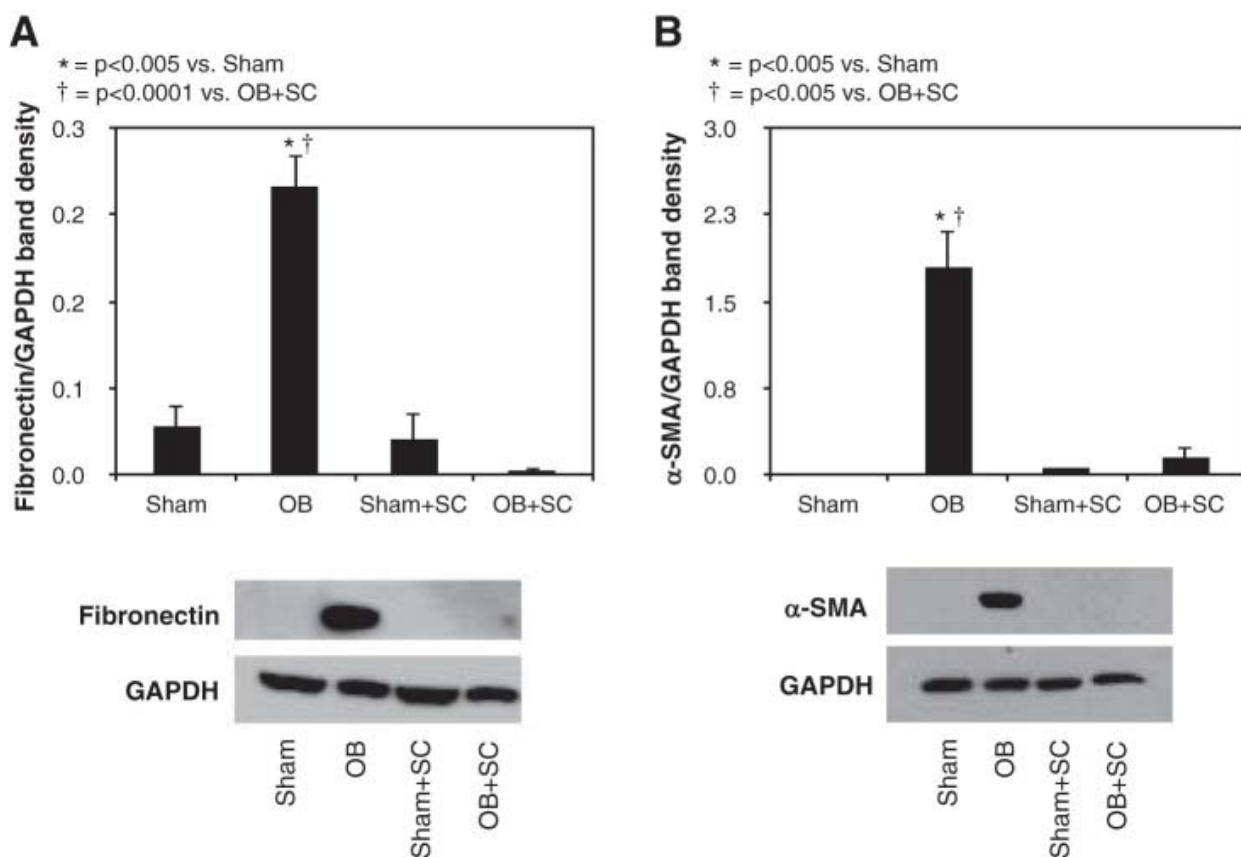
35. Tögel F, Hu Z, Weiss K, Isaac J, Lange C, Westenfelder C.. Administered mesenchymal stem cells protect against ischemic acute renal failure through differentiation-independent mechanisms. *Am J Physiol Renal Physiol* 289: F31–F42, 2005. doi:10.1152/ajprenal.00007.2005. [PubMed: 15713913]
36. Tögel F, Isaac J, Hu Z, Weiss K, Westenfelder C.. Renal SDF-1 signals mobilization and homing of CXCR4-positive cells to the kidney after ischemic injury. *Kidney Int* 67: 1772–1784, 2005. doi:10.1111/j.1523-1755.2005.00275.x. [PubMed: 15840024]
37. Tögel FE, Westenfelder C.. Kidney protection and regeneration following acute injury: progress through stem cell therapy. *Am J Kidney Dis* 60: 1012–1022, 2012. doi:10.1053/j.ajkd.2012.08.034. [PubMed: 23036928]
38. van Koppen A, Joles JA, van Balkom BW, Lim SK, de Kleijn D, Giles RH, Verhaar MC.. Human embryonic mesenchymal stem cell-derived conditioned medium rescues kidney function in rats with established chronic kidney disease. *PLoS One* 7: e38746, 2012. doi:10.1371/journal.pone.0038746. [PMCID: PMC3378606] [PubMed: 22723882]
39. Visse R, Nagase H.. Matrix metalloproteinases and tissue inhibitors of metalloproteinases: structure, function, and biochemistry. *Circ Res* 92: 827–839, 2003. doi:10.1161/01.RES.0000070112.80711.3D. [PubMed: 12730128]
40. Wang L, Luo J, He S.. Induction of MMP-9 release from human dermal fibroblasts by thrombin: involvement of JAK/STAT3 signaling pathway in MMP-9 release. *BMC Cell Biol* 8: 14, 2007. doi:10.1186/1471-2121-8-14. [PMCID: PMC1876221] [PubMed: 17480240]
41. Wang X, Zhou Y, Tan R, Xiong M, He W, Fang L, Wen P, Jiang L, Yang J.. Mice lacking the matrix metalloproteinase-9 gene reduce renal interstitial fibrosis in obstructive nephropathy. *Am J Physiol Renal Physiol* 299: F973–F982, 2010. doi:10.1152/ajprenal.00216.2010. [PubMed: 20844022]
42. Westenfelder C, Tögel FE.. Protective actions of administered mesenchymal stem cells in acute kidney injury: relevance to clinical trials. *Kidney Int Suppl* (2011) 1: 103–106, 2011. doi:10.1038/kisup.2011.24. [PMCID: PMC4089688] [PubMed: 25018910]
43. Yang J, Shultz RW, Mars WM, Wegner RE, Li Y, Dai C, Nejak K, Liu Y.. Disruption of tissue-type plasminogen activator gene in mice reduces renal interstitial fibrosis in obstructive nephropathy. *J Clin Invest* 110: 1525–1538, 2002. doi:10.1172/JCI0216219. [PMCID: PMC151817] [PubMed: 12438450]
44. Zeisberg M, Bonner G, Maeshima Y, Colorado P, Müller GA, Strutz F, Kalluri R.. Renal fibrosis: collagen composition and assembly regulates epithelial-mesenchymal transdifferentiation. *Am J Pathol* 159: 1313–1321, 2001. doi:10.1016/S0002-9440(10)62518-7. [PMCID: PMC1850511] [PubMed: 11583959]
45. Zheng G, Lyons JG, Tan TK, Wang Y, Hsu TT, Min D, Succar L, Rangan GK, Hu M, Henderson BR, Alexander SI, Harris DC.. Disruption of E-cadherin by matrix metalloproteinase directly mediates epithelial-mesenchymal transition downstream of transforming growth factor-beta1 in renal tubular epithelial cells. *Am J Pathol* 175: 580–591, 2009. doi:10.2353/ajpath.2009.080983. [PMCID: PMC2716958] [PubMed: 19590041]
46. Zhu XY, Urbieto-Caceres V, Krier JD, Textor SC, Lerman A, Lerman LO.. Mesenchymal stem cells and endothelial progenitor cells decrease renal injury in experimental swine renal artery stenosis through different mechanisms. *Stem Cells* 31: 117–125, 2013. doi:10.1002/stem.1263. [PMCID: PMC3528811] [PubMed: 23097349]

Fig. 1.



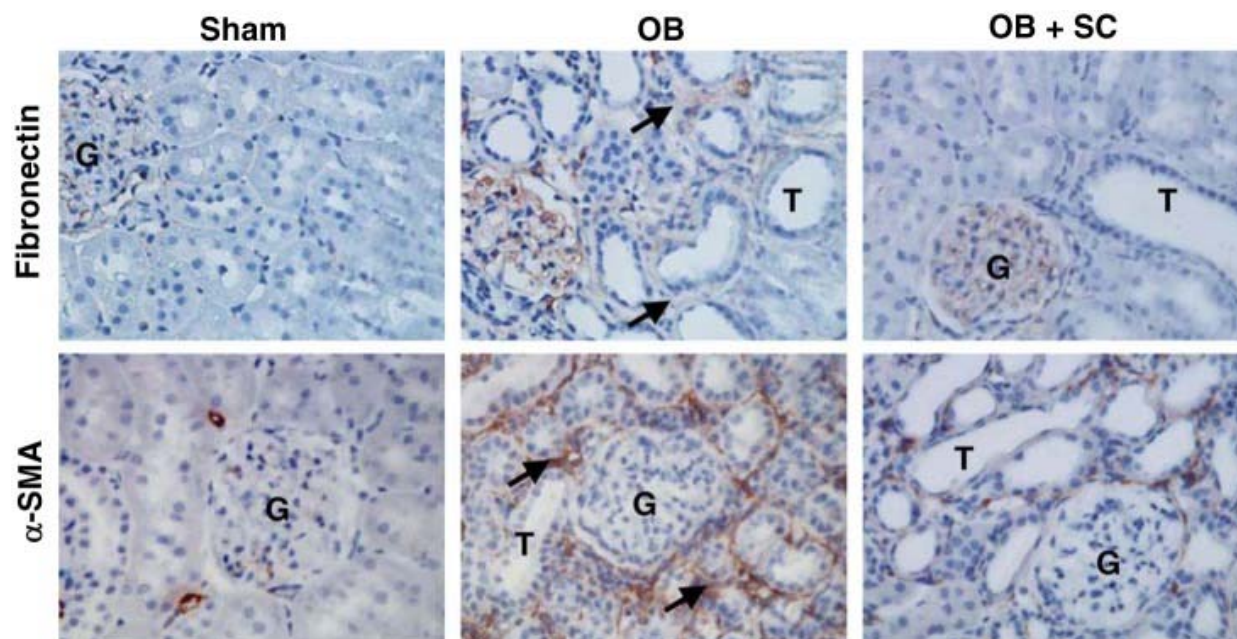
Quantitative collagen I and III mRNA expression and Masson's trichrome staining following unilateral ureteral obstruction (UUO). *A*: quantitative collagen I mRNA expression represented as a percentage of β -actin in animals exposed to sham operation in the presence of vehicle (sham) or exogenous mesenchymal stem cells (MSCs) (sham + SC), or 4 wk of UUO in the presence of vehicle (OB) or MSCs (OB + SC). *B*: quantitative collagen III mRNA expression represented as a percentage of β -actin in animals exposed to sham operation in the presence of vehicle or exogenous MSCs, or 4 wk of UUO in the presence of vehicle or MSCs. *C*: images depicting collagen deposition (blue stain; arrows) in animals exposed to sham operation or 4 wk of UUO in the presence of vehicle or MSCs. T, tubule; G, glomerulus. Magnification $\times 400$.

Fig. 2.



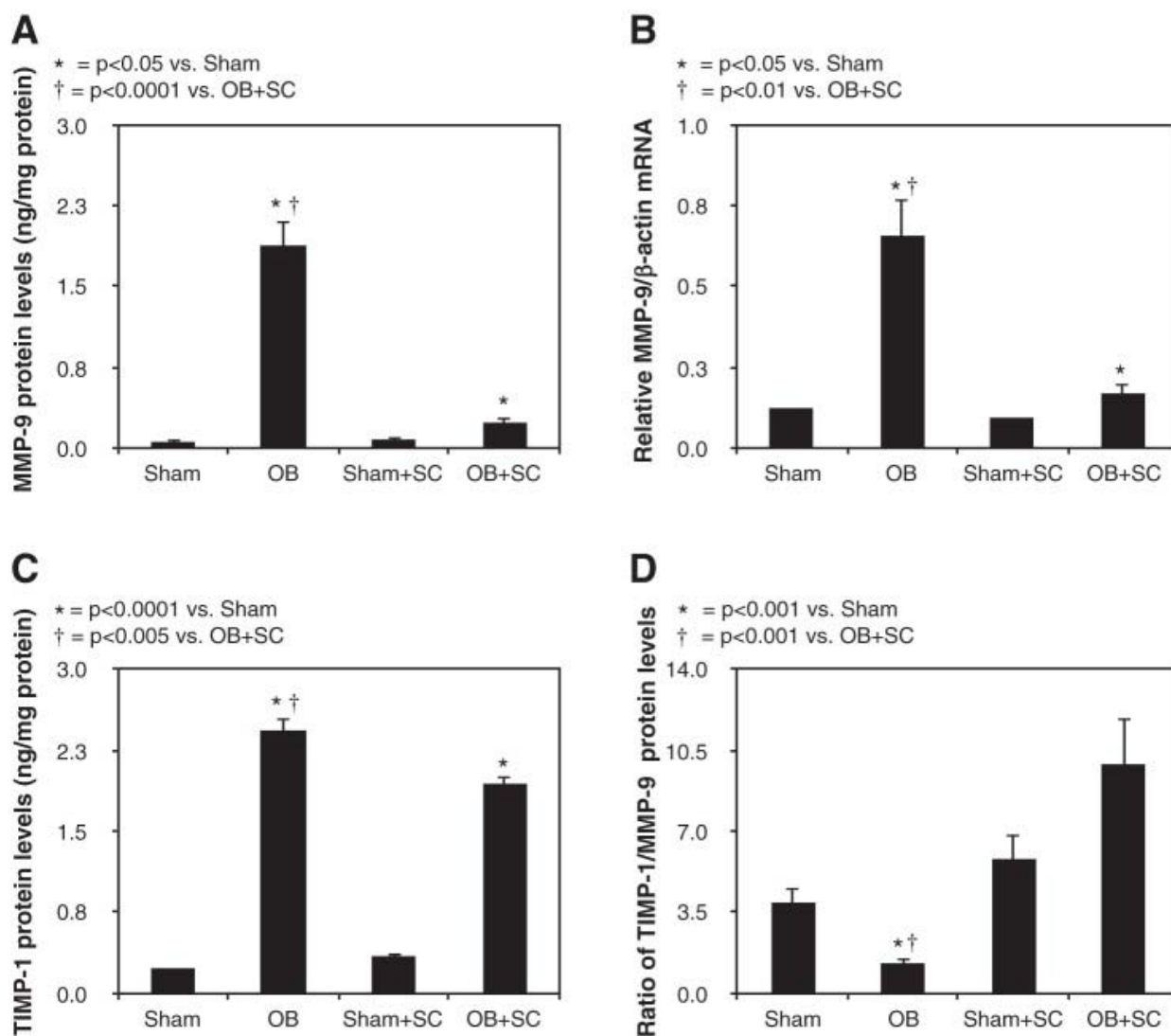
Renal cortical fibronectin and α -smooth muscle actin (α -SMA) expression following UUO. *A*: gel photograph and densitometric analysis of fibronectin expression represented as a percentage of GAPDH in animals exposed to sham operation in the presence of vehicle or exogenous MSCs, or 4 wk of UUO in the presence of vehicle or MSCs. *B*: gel photograph and densitometric analysis of α -SMA expression represented as a percentage of GAPDH in animals exposed to sham operation in the presence of vehicle or exogenous MSCs, or 4 wk of UUO in the presence of vehicle or MSCs.

Fig. 3.

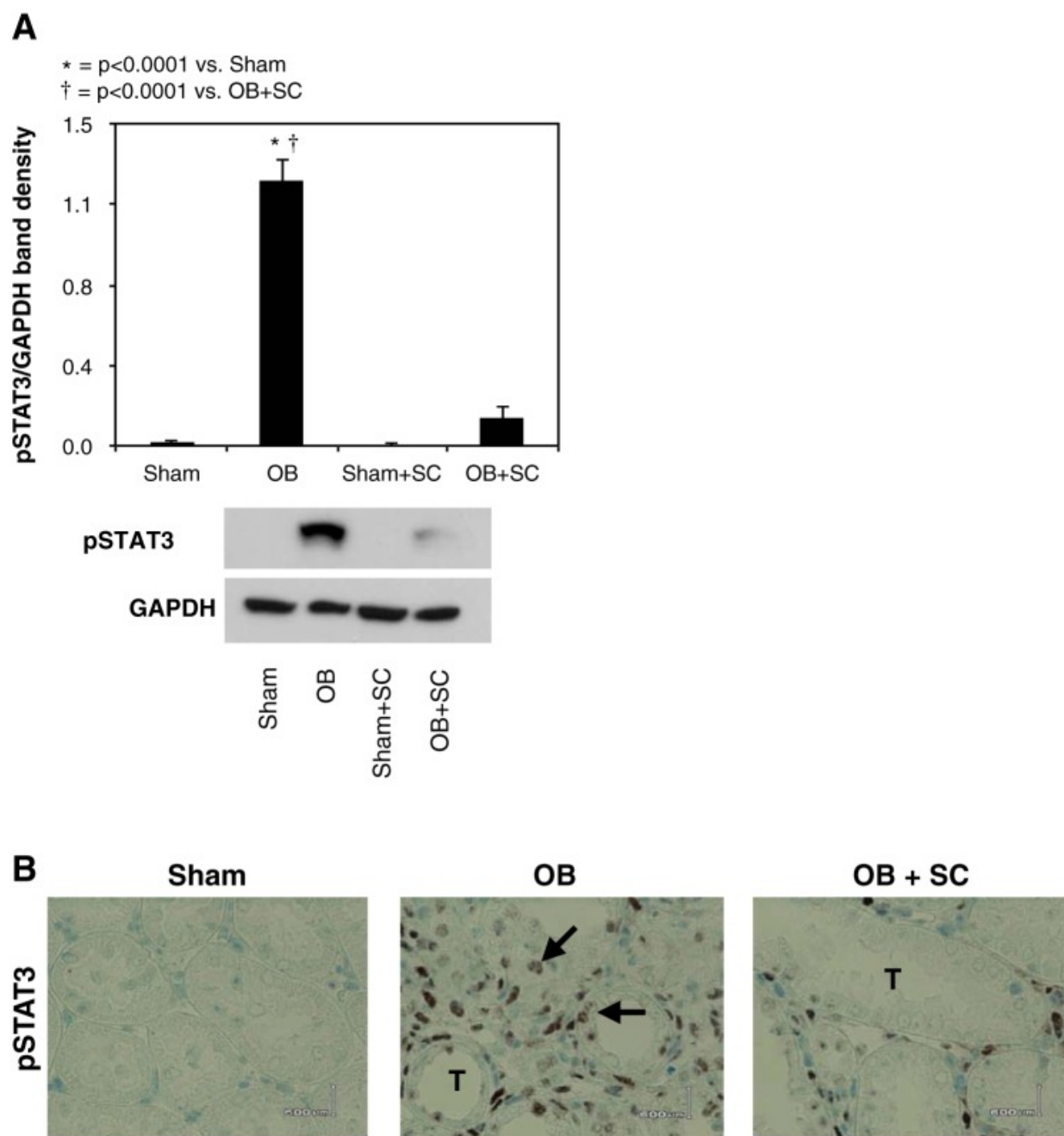


Renal cortical fibronectin and α -SMA deposition following UUO. Photographs (magnification $\times 400$) depicting renal cortical fibronectin and α -SMA deposition (brown stain; arrows) in animals exposed to sham operation or 4 wk of UUO in the presence of vehicle or MSCs. Magnification $\times 400$.

Fig. 4.



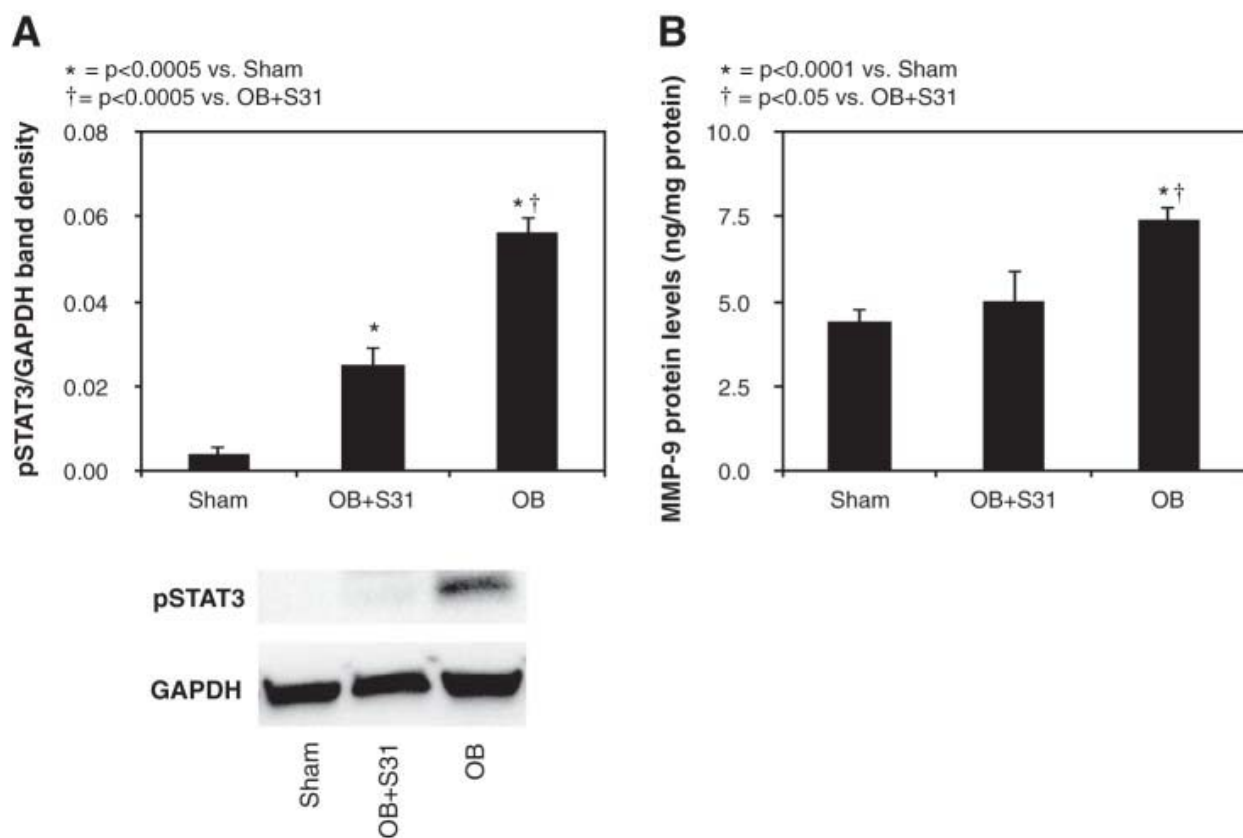
Renal cortical matrix metalloproteinase 9 (MMP-9) and tissue inhibitor of matrix metalloproteinase-1 (TIMP-1) protein expression and quantitative MMP-9 mRNA expression following UUO. *A*: MMP-9 protein levels in animals exposed to sham operation in the presence of vehicle or exogenous MSCs, or 4 wk of UUO in the presence of vehicle or MSCs. *B*: quantitative MMP-9 mRNA expression represented as a percentage of β -actin in animals exposed to sham operation in the presence of vehicle or exogenous MSCs, or 4 wk of UUO in the presence of vehicle or MSCs. *C*: TIMP-1 protein levels in animals exposed to sham operation in the presence of vehicle or exogenous MSCs, or 4 wk of UUO in the presence of vehicle or MSCs. *D*: ratio of TIMP-1/MMP-9 protein levels in animals exposed to sham operation in the presence of vehicle or exogenous MSCs, or 4 wk of UUO in the presence of vehicle or MSCs.

Fig. 5.

[Open in a separate window](#)

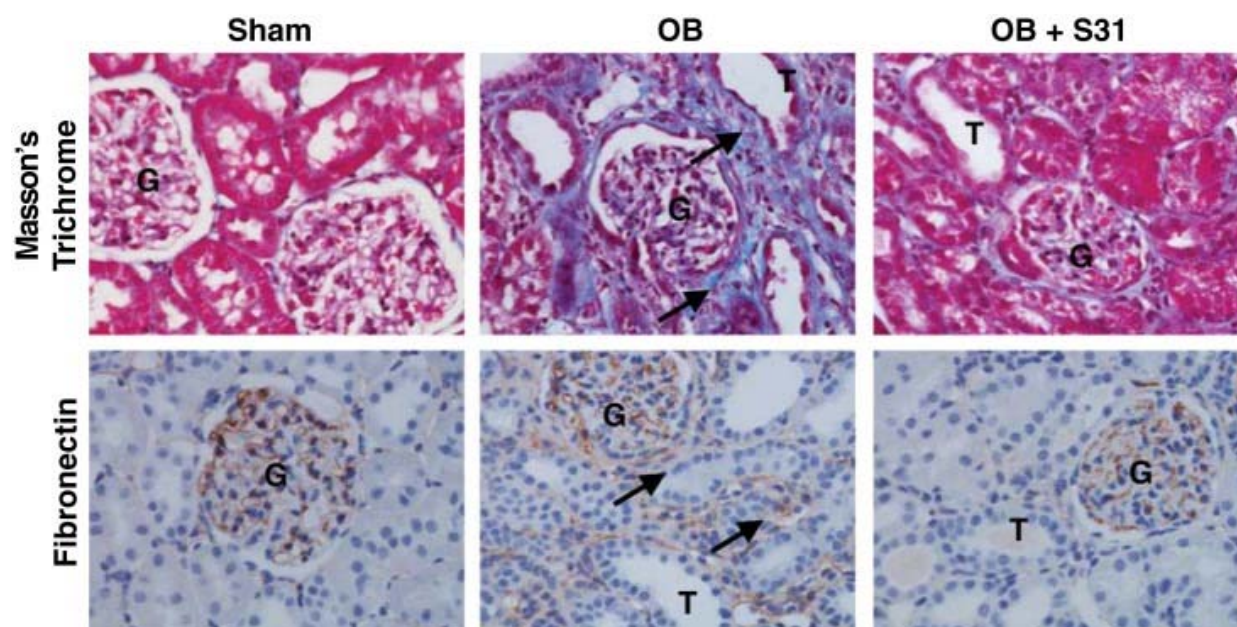
Renal cortical active STAT3 (p-STAT3) protein expression and immunolocalization following UUO. *A*: gel photograph and densitometric analysis of p-STAT3 expression represented as a percentage of GAPDH in animals exposed to sham operation in the presence of vehicle or exogenous MSCs, or 4 wk of UUO in the presence of vehicle or MSCs. *B*: photographs depicting renal cortical STAT3 (brown stain; arrows) in animals exposed to sham operation or 4 wk of UUO in the presence of vehicle or MSCs. Magnification $\times 400$.

Fig. 6.



Effect of S3I-201 on renal cortical p-STAT3 and MMP-9 protein expression following UUU. *A*: gel photograph and densitometric analysis of p-STAT3 expression represented as a percentage of GAPDH in animals exposed to sham operation or 2 wk of UUU in the presence of vehicle or S3I-201 (OB + S3I-201). *B*: MMP-9 protein levels in animals exposed to sham operation or 2 wk of UUU in the presence of vehicle or S3I-201.

Fig. 7.



Effect of S3I-201 on renal cortical collagen and fibronectin deposition following UUO. Photographs (magnification $\times 400$) depicting renal cortical collagen deposition (Masson's trichrome, blue stain, arrows) and fibronectin deposition (brown stain, arrow) in animals exposed to sham operation (sham) or 2 wk of UUO in the presence of vehicle (OB) or S3I-201 (OB + S3I-201). Magnification $\times 400$.

Articles from American Journal of Physiology - Renal Physiology are provided here courtesy of **American Physiological Society**